Volume 18, Number 5, 2025. pp. 573-581

Jordan Journal of Physics

ARTICLE

Spectroscopic Diagnostic and Preparation of CuSi Plasma Produced Via Plasma Jet

Wadaa S. Hussein[a], **Riyam N. Muhsen**[a], **Kadhim A. Aadim**[a] and **Abdulrhman H. Shaker**[b]

[a] *Department of Physics, College of Science, University of Baghdad, Baghdad, Iraq.*
[b] *Al Hikma university college, Baghdad, Iraq.*

Doi: **https://doi.org/10.47011/18.5.2**
Received on: 21/02/2024; *Accepted on: 28/01/2025*

Abstract: Copper silica (CuSi) plasma was generated under atmospheric pressure using argon gas by immersing a piece of (Si) metal in the prepared nano-Cu liquid for periods of 6 and 8 min. Then, a spectroscopic diagnosis of the generated plasma was performed at a constant applied voltage of 11 kV and a frequency of 50 kHz under direct-current conditions, with the argon flow rate varied between 0.5 and 2 L/min. Changing the duration of immersion within the nano-Cu liquid and the flow rate of argon affected the intensity of the resulting spectral peaks. The generated plasma had the following parameters: T_e values of 3.732 – 4.981 eV and 1.220 – 1.396 eV, and n_e values of $2.700 \times 10^{18} - 3.588 \times 10^{18}$ cm^3 and $1.290 \times 10^{18} - 2.074 \times 10^{18}$ cm^3 for the two times used. When CuSi nanoparticles (NPs) were synthesized under the same laboratory conditions, with the argon flow rate fixed at 2 L/min, the energy gap was 3.74 eV, prepared by Si for 6 min in Cu-liquid for 6 min, and 3.62 eV, prepared of Si for 6 min in Cu-liquid for 8 min. The results showed that the Cu-liquid increased the electrical conductivity in the CuSi cold jet plasma system, which affected the values of the plasma parameters and the synthesis of CuSi NPs as a result of increased energy gain, which accelerated and increased the electron process and ultimately increased the ionisation process.

Keywords: CuSi cold plasma jet, CuSi nanoparticle, Optical emission spectroscopy (OES), Spectral diagnostics, Silicon-copper plasma.

1. Introduction

Plasma science is one of the most extensively studied and developed fields in the modern era. The atmospheric pressure plasma jet remains an advanced method for generating cold plasma, and it is widely used in scientific applications [1, 2]. This is also called a cold plasma jet [3]. Cold jet plasma is formed by the ionisation of molecules or atoms of the substance at a certain temperature, which then becomes a highly reactive gas containing radicals, electrons, extremely active free ions, and electric fields [4]. Both noble gases, such as helium and argon, and chemically active gases, such as nitrogen and oxygen, can be used in this production process [5]. Non-thermal plasma jets are effective tools for industrial, medical, and biological uses due to their ability to interact with cells, tissues, and various industrial applications easily and without significant effects [6, 7]. Each type of plasma possesses distinct characteristics that determine its suitability for specific applications [8]. Temperature and density are the most important dynamics in plasma, and they enable us to predict the particle velocity distributions and relative energy levels [9].

To measure the plasma parameters such as electron temperature (T_e) and electron density (n_e), optical emission spectroscopy (OES) is adopted [10]. This technique allows for plasma diagnostics without disturbing its structure, condition, or shape [11]. The method's principal

Corresponding Author: Abdulrhman H. Shaker **Email**: Abd.Hamed2204m@sc.uobaghdad. edu.iq

work is calculating the radiated optical emission from the produced plasma, which represents its characteristics in an environment of chemical, ionic, and molecular radiation [12, 13]. As ionised plasma particles interact with each other and emit radiation, three high-speed electronic transitions that control collision excitation and ionisation can occur: boundary transitions, important transitions, and free transitions [14]. A band or spectral line is formed from the emitted light as electrons pass through different levels in it, thereby resulting in the energetic gas molecules, ions, and atoms emitting radiation [15].

To determine the properties of a plasma, its parameters must be calculated. As noted above, the temperature and density of the electrons are considered among the most important properties, from which the remainder of the parameters can be derived. The temperature of the plasma in local thermal equilibrium can be calculated using the following equation [16]:

$$T_e = \frac{(E_2 - E_1)}{k \ln\frac{(I_1\lambda_1 A_2 g_2)}{(I_2\lambda_2 A_1 g_1)}} \quad (1)$$

where A_1g_1 is the transition strength of the first wavelength, A_2g_2 is the transition strength of the second wavelengths, k is Boltzmann's constant, I_1 and I_2 are the peak intensity of the first and second wavelength of the plasma spectrum, E_1 is the peak energy of the first wavelength, and E_2 is the peak energy of the second wavelength in the resulting plasma spectrum. Moreover, A is the transition probability for spontaneous emission from an upper energy level to a lower level, and g is the statistical weight of the upper level [17]. Here, the unit of measurement is eV.

From the Saha-Boltzmann equation, which depends on spectral lines, the plasma electron density can be calculated as follows [16]:

$$n_e = \frac{I_1}{I_2^*} 6.04 \times 10^{21} (T_e)^{3/2} e^{\frac{(E_1 - E_2 - X_z)}{kT_e}} \quad (2)$$

where I_1 and I_2 are the peak intensity of the first and second wavelength of the plasma spectrum, E_1 and E_2 are the peak energy of the wavelengths, as defined above, and X_z represents the amount of ionisation energy. Here, the unit of measurement is cm^{-3}.

$$I_2^* = \frac{I_2\lambda_2}{g_2 A_2} \quad (3)$$

The synthesis of nanoparticles (NPs) has been widely investigated because their extremely small atomic and molecular dimensions impart properties that differ significantly from those of bulk materials [18]. The potential of the NP technology lies in the fact that increasing the ratio of particle area to volume gives different and variable properties [19].

This work aims to determine copper-silica (CuSi) plasma parameters when using a variable argon gas flow rate of 0.52 L/min, and a high voltage of 11 kV as a direct current power supply, and to measure the energy gap of the CuSi compound. To this end, a spectroscopic diagnostic method is adopted.

2. Experimental Setup

Figure 1 shows a non-thermal plasma jet system based on argon gas using DC and an applied voltage of 11 kV. A slice of Cu measuring 6 cm in length and 1 cm in width was immersed in a non-ionic liquid inside a 10 ml beaker connected to the positive pole. The electrically conductive plasma jet needle was connected at one end to a gas flow meter and an argon gas bottle and connected by a metal wire to the negative pole. When the system was turned on, and the jetting process began, plasma was produced, as shown in Fig. 2. The nano-Cu liquid was prepared for durations of 6 and 8 min at an argon gas flow rate of 2 L/min, during which the gas interacted with the non-ionic liquid and the immersed metal. The gas molecules interacted with the liquid in the beaker and produced a series of reactions on the metal surface. As a result of the production of NPs, the liquid changed to a brown color, and it became darker as the preparation time increased. The plasma needle was almost perpendicular to the beaker in which the water was placed, and a metal holder was placed on the beaker to control the distance of the flowing plasma column, which was measured during the experimental conditions at 2.35 cm (Fig. 2).

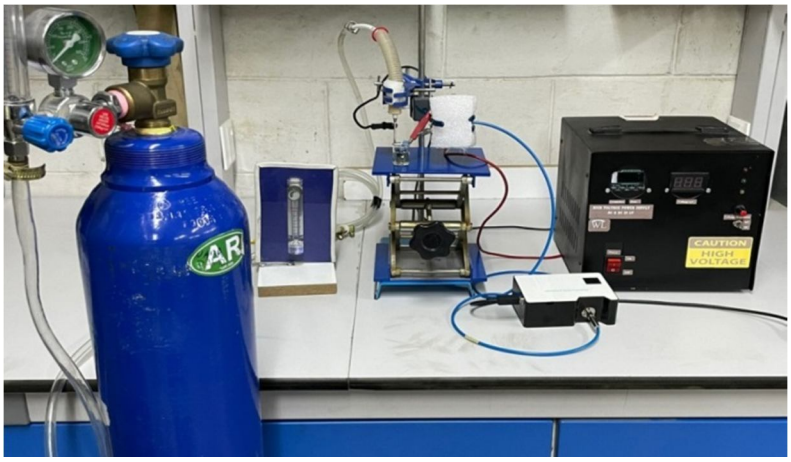

FIG. 1. Configuration of the non-thermal plasma jets system, spectrometer, and electronic controller.

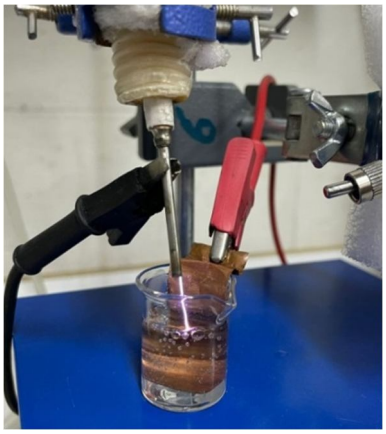

FIG. 2. Cold plasma jet, its interaction with the liquid and the metal surface, and electrode connection.

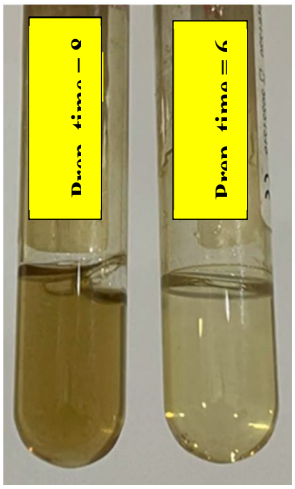

FIG. 3. Image of the synthesized Cu nanoparticles by the atmospheric plasma jet prepared for specific time periods (6 and 8 min).

In the next step, a slide of silicon metal with a length of 4 cm and a width of 1 cm (connected to the anode electrode) was immersed in the previously prepared nano-Cu liquid, using DC and an applied voltage of 11 kV at an argon gas flow of 0.52 L/min from the tip of the plasma jet (connected to the cathode). Plasma was produced, and its parameters were measured using a spectrophotometer. Using the same plasma production mechanism with an argon gas flow rate of 2 L/min for 6 min, CuSi NPs were produced. The color of the liquid changed to light brown when NPs of Si were produced in the nano-Cu liquid prepared with a time of 6 min for both Cu and Si. The color of the liquid changed to light green when NPs were produced in the liquid prepared for 8 min for Cu and 6 min for Si, as shown in Fig. 4.

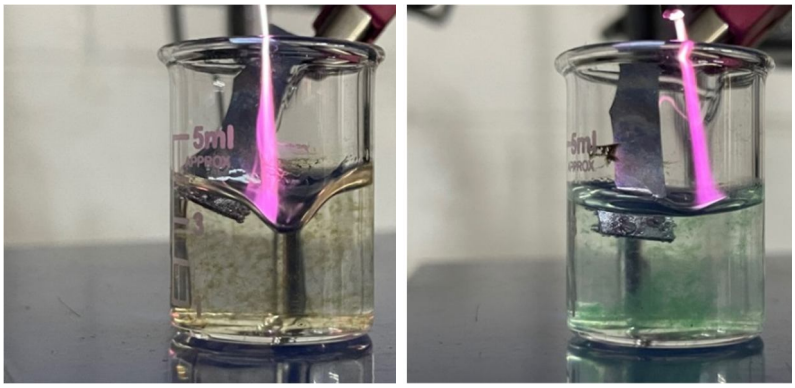

(a) (b)

FIG. 4. Images of nanoparticle liquid samples manufactured for CuSi by atmospheric plasma jet: (a) 6 min for Cu and 6 min for Si; (b) 8 min for Cu and 6 min for Si.

The optical properties (absorption and energy gap) of the NPs produced by the plasma jet were measured using a UV-visible spectroscopy device (UV-Vis 1800, Shimadzu), which is considered the practical method for determining pure substances [20]. Optical characterization provides important physical information about the material, such as its absorption behavior and band-gap energy. These parameters were determined using Planck's relation and the Tauc relation for direct electronic transitions [21]:

$$E_g^{opt.} = \frac{hc}{\lambda_{cut}} = \frac{1240}{\lambda_{cut}} \quad (4)$$

and

$$(\alpha h)^r = A\left(h - E_g\right) \quad (5)$$

In Eq. (4), E_g represents the optical energy gap, h = m (6.626l × 10^{34} J.s) is Planck's constant, c = (3×10^8 m/s) is the light velocity in a vacuum, and λ_{cut} represents the cut-off wavelength corresponding to the optical band gap. In Eq. (5), α is the absorption coefficient, h is Planck's constant, υ is the incident photon frequency, A is a constant equal to 0.9, and r is a value depending on the nature of the transition type (r = 2) for an allowed direct transition.

3. Results and Discussion

Optical Emission Spectrum (OES)

The optical emission spectrum used in the plasma jet system produced by Cu and Si under atmospheric pressure conditions, and the effect of the applied voltage of 11 kV and the variable argon gas flow rate (0.52 L/min) on the properties and parameters of the plasma were studied. Information was collected, and Si plasma emissions were examined using a fibre-optic beam connected to a spectrometer. This provided information on the decay of the excited emissions in the plasma. The physical properties of the metals employed and the laboratory operating conditions significantly affected the observed spectral emission lines and, consequently, the accuracy of the plasma-parameter calculations. As shown in Fig. 5, the spectroscopic diagnosis of the argon plasma jet operating under DC conditions with a silicon metal immersed in nano-Cu liquid prepared for 6 min revealed several emission peaks. Ar +2 peaks were observed at wavelengths of 223.54, 244.04, 253.57, 335.56, 396.98, 706.61, 810.54, and 839.85 nm. It was found that five Cu +2 peaks appeared at 226.35, 294.77, 419.27, 696.73, and 809.62 nm, while three CuSi +2 peaks were detected at 308.6, 379.42, and 671.99 nm. Under identical operating conditions, but using nano-Cu liquid prepared for 8 min, the spectroscopic analysis showed Ar +2 emission peaks at 223.54, 244.05, 253.57, 335.56, 396.98, 706.61, 810.54, and 839.85 nm. The Cu +2 emission peaks were observed at 280.90, 308.05, 355.79, 380.24, and 749.91 nm, while CuSi +2 peaks appeared at 211.41, 234.23, 378.61, and 671.74 nm. In addition, Si emission lines were detected at 613.22 and 762.83 nm.

It was observed that the intensities of the emission peaks increased when Si plasma was generated using nano-Cu liquid prepared for 8 min. This enhancement can be attributed to the increased electrical conductivity of the nanoliquid, which promotes more effective interactions between argon gas molecules and the silicon metal surface. As a result, the ionization levels of electrons, ions, and free radicals increased. These findings are consistent with previous studies [22], which reported that the use of Cu nanoparticles in liquid media enhances electrical conductivity and accelerates

plasma formation. Accordingly, the plasma behavior and parameter trends observed in the present study are in good agreement with those reported in Ref. [22].

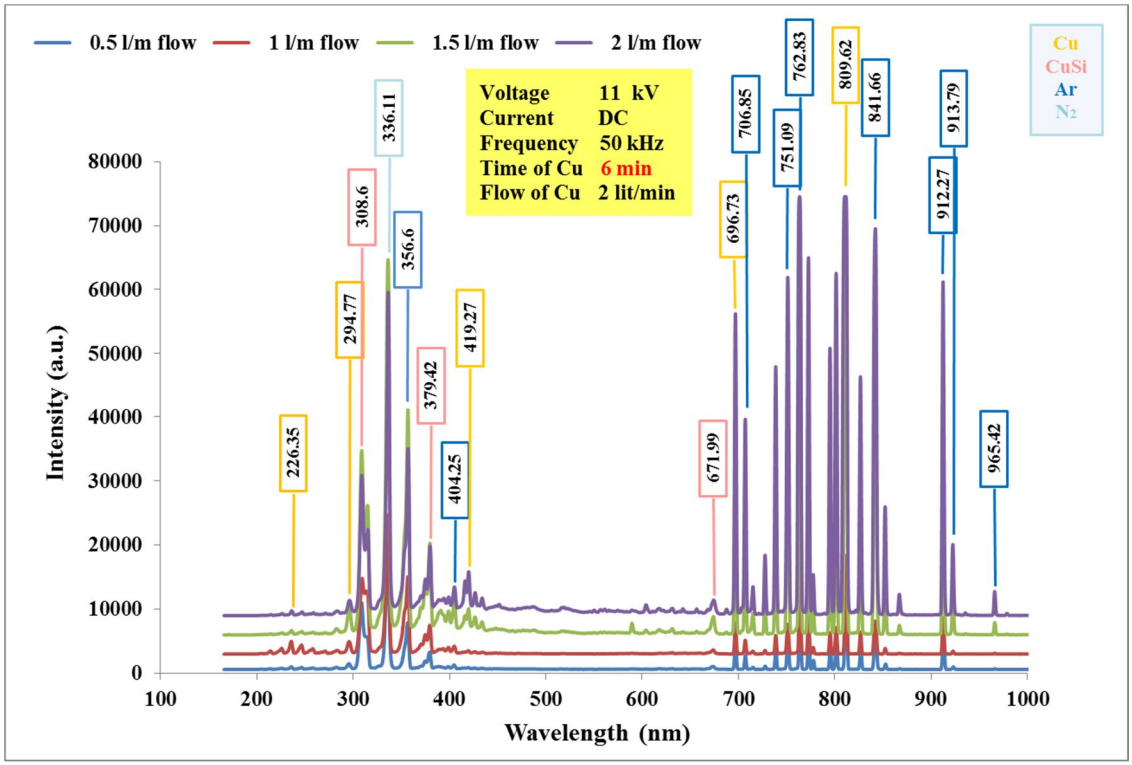

FIG. 5. Plasma emission spectra of Si in nano-Cu liquid prepared for 6 min in a non-ionic liquid at various argon gas flow rates.

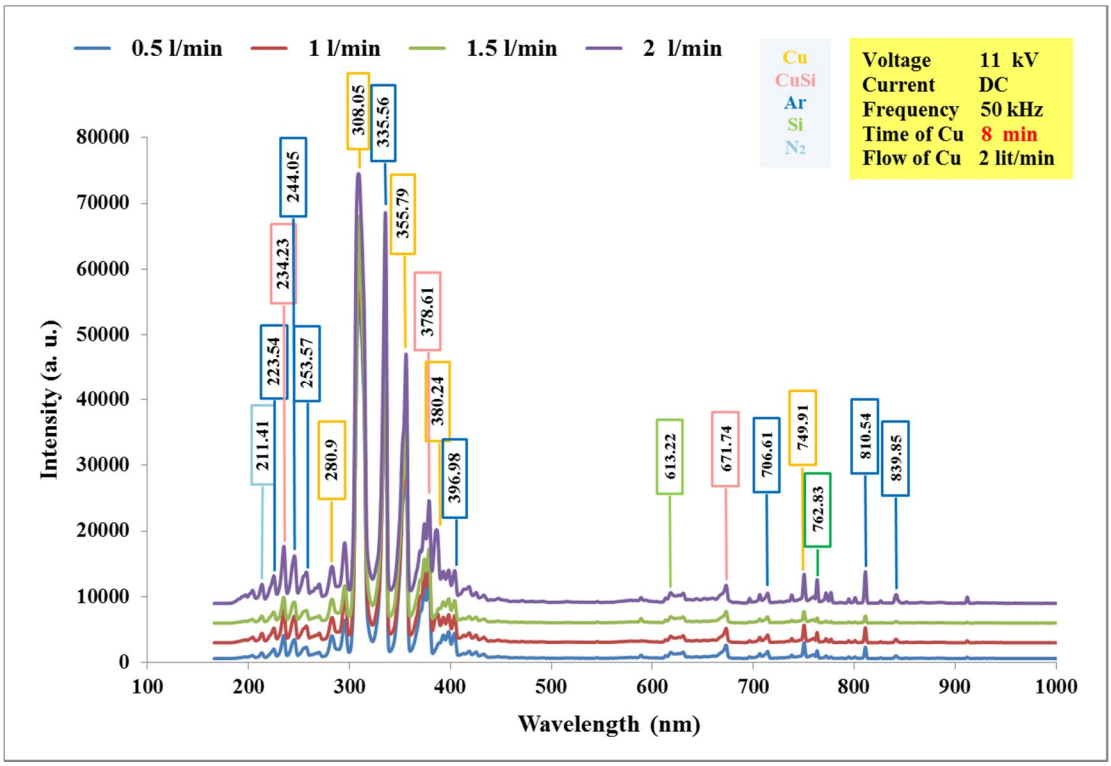

FIG. 6. Plasma emission spectra of Si in nano-Cu liquid prepared for 8 min in a non-ionic liquid at various argon gas flow rates.

Using Eq. (3), the parameters of CuSi plasma produced under two different Cu nanoliquid preparation times (6 and 8 min) were calculated. As Fig. 7 shows, T_e and n_e increased to 3.732 4.981 eV and 2.700 × 10^{18} - 3.588 × 10^{18} cm^3 with the increase in the flow rate of argon gas

(0.5–2 L/min) for Si-anode plasma in the nano-Cu liquid (6 min). This increase is attributed to enhanced collisions between the argon gas molecules and the surface of the nano-Cu liquid containing the immersed Si plate. This led to an increase in the ionization process, providing electrons with more energy to move from a lower level to a higher level. As the temperature increased, the electron density increased accordingly. As Fig. 8 shows, T_e and n_e increased (1.220 – 1.396 eV; 1.290 × 10^{18} 2.074 × 10^{18} cm^{3}) with the increase in the flow rate of argon gas for the Si-anode plasma in the nano-Cu liquid (8 min), which was a result of the increase in collision between the gas column and the surface of the liquid in which the metal was immersed. Finally, there was an increase in plasma ionization processes, with the observed behavior similar to that observed in previous research [16]. It is the increase in the value of plasma parameters with different metals.

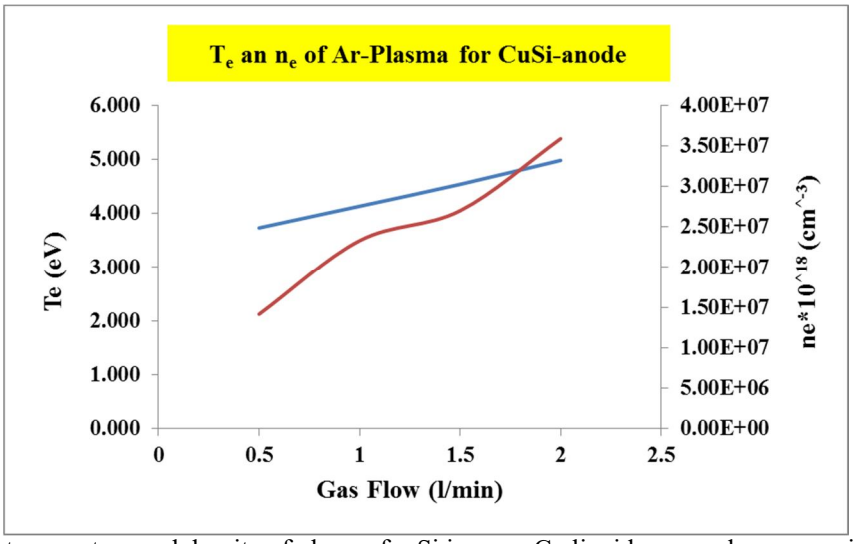

FIG. 7. Electron temperature and density of plasma for Si in nano-Cu liquid prepared over a period of 6 min as a function of argon gas flow rate.

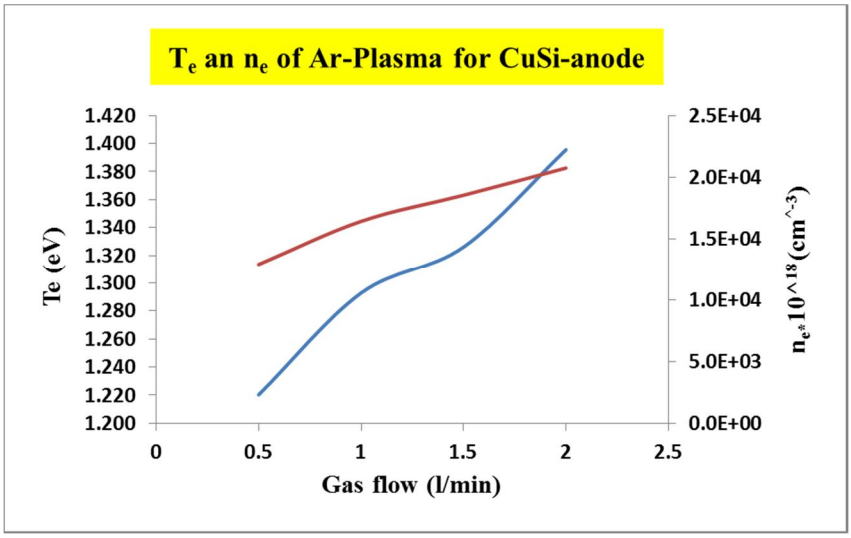

FIG. 8. Electron temperature and density of plasma for Si in nano-Cu liquid prepared over a period of 8 min as a function of argon gas flow rate.

Immersion of the silicon metal sheet in the nano-Cu liquid increased the collision process of argon gas atoms with the liquid surface, which led to an increase in the excitation of electrons and the speed of their transition to a higher level, thus increasing their value. This led to an increase in the ionization process during the generation of the plasma column, which again was in line with previous research results, which led to an increase in the temperature and electron density of the produced plasma, and this behavior is consistent with the results of the aforementioned study [23].

Optical Properties

Figures 9 and 10 show the optical absorption spectrum of the CuSi NPs produced via the plasma jet with an applied voltage of 11 kV and a constant Ar flow rate of 2 L/min over two time periods: 6 min for both Cu and Si. Using Eqs. (4) and (5), the energy gap was calculated. From the absorption spectra, the energy gap was determined by projecting the intersection of the extrapolated linear portion of the absorption curve onto the photon energy axis. The energy gap value was estimated using the standard energy gap band estimation method, in which a straight line is drawn that settles at the horizontal axis diagonally, and were found to be 3.74, 3.62 eV. From a physical perspective, an electron requires an energy of 3.74, 3.62 eV to release a photon from the valence band to the conduction band, as the same conduction and valence bands exist in the direct band gap of the hole momentum and the electron. This result was close to that obtained in terms of value in previous research [24].

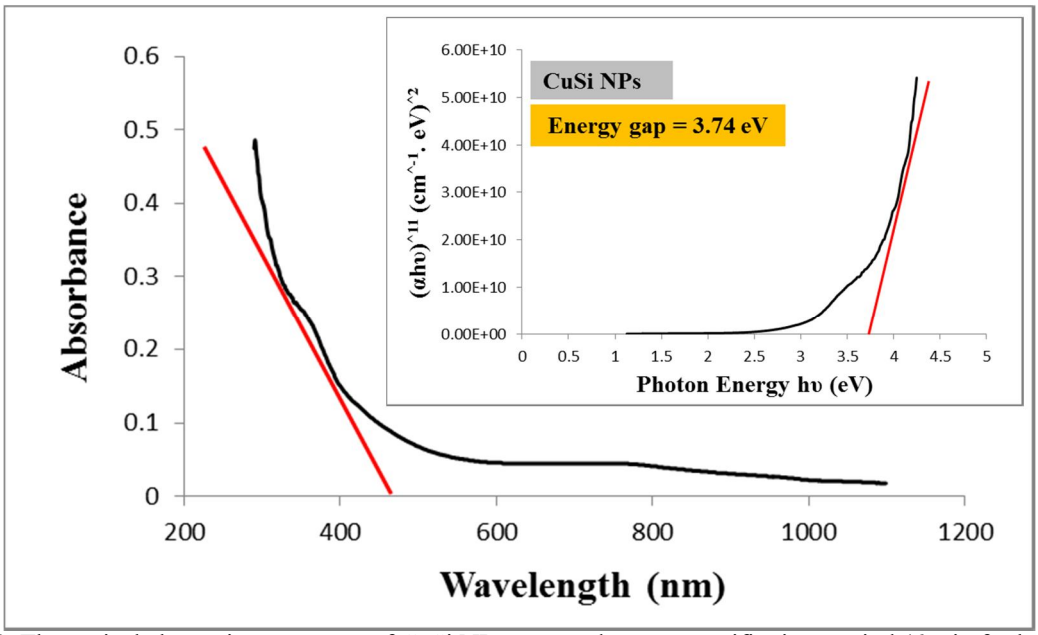

FIG. 9. The optical absorption spectrum of CuSi NPs prepared over a specific time period (6 min for both Cu and Si) along with the energy gap.

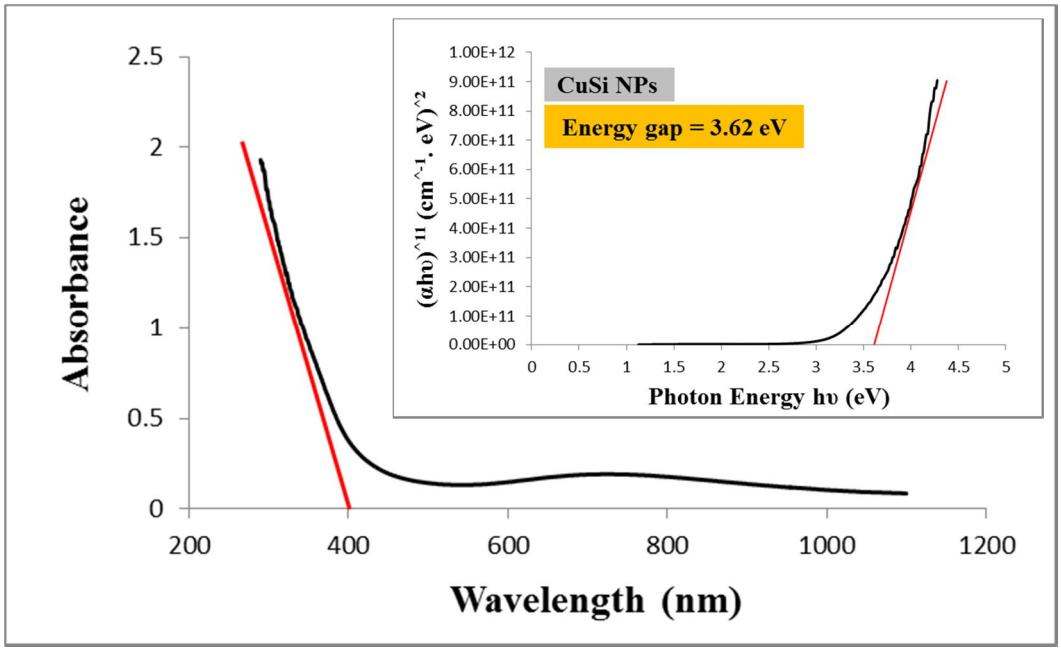

FIG. 10. The optical absorption spectrum of CuSi NPs prepared over a specific time period (8 min for Cu and 6 min for Si) along with the energy gap.

4. Conclusion

The nano-Cu liquid affected the gas ionization processes in the Ar plasma jet system, increasing the intensity of the spectral lines of Cu and Si metals. The external factors, such as the applied voltage (11 kV) and the variable gas flow rate (0.2–5 L/min), had a further effect on increasing the number of colliding gas molecules. As such, the energy supplied as a result of the high excitation process was sufficient to cause ionization, meaning that the intensity of the spectral lines increased. The spectral peaks were lower at the gas flow rate of 0.5 L/min and higher at the rate of 2 L/min, which was reflected in the plasma parameters: T_e of 3.732 – 4.981 eV and 1.220 – 1.396 eV, and n_e values of $2.700 \times 10^{18} - 3.588 \times 10^{18}$ cm^3 and $1.290 \times 10^{18} - 2.074 \times 10^{18}$ cm^3 for the two different times. The changes obtained in the plasma parameters give the generated plasma the ability to be used in different applications.

The optical properties of the Cu and Si NPs produced via Ar plasma jetting exhibited a change in optical absorption rate and energy gap value. The optical band-gap values were measured as 3.74 and 3.62 eV for the time applied in the experiment, as a result of changing the preparation time of the Cu liquid from 6 to 8 min and using it to immerse the Si metal and synthesize the Cu and Si NPs at a constant applied voltage of 11 kV and a gas flow rate of 2 L/min. This result indicates the increase in the electrical conductivity of the Cu particles and the collision process of the gas molecules with the metal surface from the moment the gas came into contact with the liquid surface to the moment its molecules collided with the Si metal surface. This was due to an increase in the uprooting of the Si particles to form the Cu and Si NPs.

5. Acknowledgment

We would like to express our gratitude and thanks to the plasma laboratory in the Physics Department, College of Science, University of Baghdad.

Statements & Declarations

The authors confirm that all information and data have been presented in this manuscript

Funding Declaration in the Manuscript

The authors did not receive support or assistance from any organization for the submitted work.

Conflicts of Interest/ Competing Interests

All authors certify that they have no affiliations with or involvement in any organization or entity with any financial interest or non-financial interest in the subject matter or materials discussed in this manuscript.

Contributions

All authors contributed to this work. Riyam N. Muhsen, Wadaa S. Hussein, Abdulrhman H. Shaker, and Kadhim A. Aadim produced the idea and method of work, and Abdulrhman, Riyam, and Wadaa conducted the practical application, calculations, and data analysis. Riyam N. Muhsen and Abdulrhman worked on writing the theoretical part. All authors contributed to writing the summary and conclusion.

References

[1] Tabares, F.L. and Junkar, I., Molecules, *26* (7) (2021) 1903.

[2] Winter, J., Brandenburg, R., and Weltmann, K.-D., Plasma Sources Sci. Technol., 24 (2015) 064001.

[3] Stryczewska, H.D. and Boiko, O., Appl. Sci., 12 (9) (2022) 4405.

[4] Moravský, L., Klas, M., and Matejčík, Š., WDS'13 Proc. Contrib. Pap., Part II, (2013), 149–153.

[5] Shaker, A.H., Aadim, K.A., and Nida, M.H., J. Opt., 53 (2024) 1273.

[6] Hameed, M.M., Al-Samarai, A.-M.E., and Aadim, K.A., Iraqi J. Sci., 61 (10) (2020) 2582.

[7] Hashim, H. et al., Mater. Lett., 373 (2024) 137077.

[8] Wang, D. and Namihira, T., Plasma Sources Sci. Technol., 29 (2020) 023001.

[9] Mohammed, R.S., Aadim, K.A., and Ahmed, K.A., Appl. Nanosci., 12 (12) (2022) 3783.

[10] Akatsuka, H., Adv. Phys.: X, 4 (1) (2019) 1592707.

[11] Zaplotnik, R., Primc, G., and Vesel, A., Appl. Sci., 11 (5) (2021) 2275.

[12] Pauna, H., Aula, M., Seehausen, J., Klung, J.-S., uttula, M., and Fabritius, T., Steel Res. Int., 91 (2020) 20000.

[13] Qusnudin, A., Kusumandari, K., and Saraswati, T.E., J. Phys.: Conf. Ser., 1825 (2021) 012072.

[14] Aadim, K.A. and Yousef, A.A., Iraqi J. Sci., 95 (1C) (2018) 494.

[15] Samarkhanov, K., Khasenov, M., Batyrbekov, E., Kenzhina, I., Sapatayevn, Y., and Bochkov, V., Sci. Technol. Nucl. Install., 2020 (2020) 8891891.

[16] Tabares, F.L. and Junkar, I., Molecules, 26, 1903, (2021).

[17] Shaker, A.H., Aadim, K.A., Iraqi J. Appl. Phys., 20 (3B) (2024) 675.

[18] Afkhami, A. and Norooz-Asl, R., Colloids Surf. A Physicochem. Eng. Asp., 346 (1–3) (2009) 52.

[19] Imran, H.J., Hubeatir, K.A., and Aadim, K.A., Sci. Rep., 13 (1) (2023) 5441.

[20] Akash, M.S.H. and Rehman, K., "Ultraviolet-Visible (UV-VIS) Spectroscopy", In: "Essentials of Pharmaceutical Analysis", (Springer, Singapore, 2020), pp 29–56.

[21] Baniya, H.B., Shrestha, R., Guragain, R.P., Kshetri, M.B., Pandey, B.P., and Subedi, D.P., Int. J. Polym. Sci., 2020 (2020) 9247642.

[22] Hussein, T.S., Ahmed, A.F., and Aadim, K.A., Iraqi J. Sci., 63 (2) (2022) 548.

[23] Shehab, M.M. and Aadim, K.A., Iraqi J. Sci., 62 (9) (2021) 2948.

[24] Pligovka, A., Hoha, A., Turavets, U., Poznyak, A., Zakharau, Y., Mater. Today: Proc., 37 (4) (2021) A8.